

TabSieve: Explicit In-Table Evidence Selection for Tabular Prediction

Yongyao Wang*, Ziqi Miao*, Lu Yang, Haonan Jia, Wenting Yan, Chen Qian, Lijun Li

Gaoling School of Artificial Intelligence, Renmin University of China

Shanghai AI Laboratory

The Hong Kong Polytechnic University
Zhejiang University

Tabular prediction can benefit from in-table rows as few-shot evidence, yet existing tabular models typically perform instance-wise inference and LLM-based prompting is often brittle. Models do not consistently leverage relevant rows, and noisy context can degrade performance. To address this challenge, we propose TabSieve, a select-then-predict framework that makes evidence usage explicit and auditable. Given a table and a query row, TabSieve first selects a small set of informative rows as evidence and then predicts the missing target conditioned on the selected evidence. To enable this capability, we construct TabSieve-SFT-40K by synthesizing high-quality reasoning trajectories from 331 real tables using a strong teacher model with strict filtering. Furthermore, we introduce TAB-GRPO, a reinforcement learning recipe that jointly optimizes evidence selection and prediction correctness with separate rewards, and stabilizes mixed regression and classification training via dynamic task-advantage balancing. Experiments on a held-out benchmark of 75 classification and 52 regression tables show that TabSieve consistently improves performance across shot budgets, with average gains of 2.92% on classification and 4.45% on regression over the second-best baseline. Further analysis indicates that TabSieve concentrates more attention on the selected evidence, which improves robustness to noisy context.

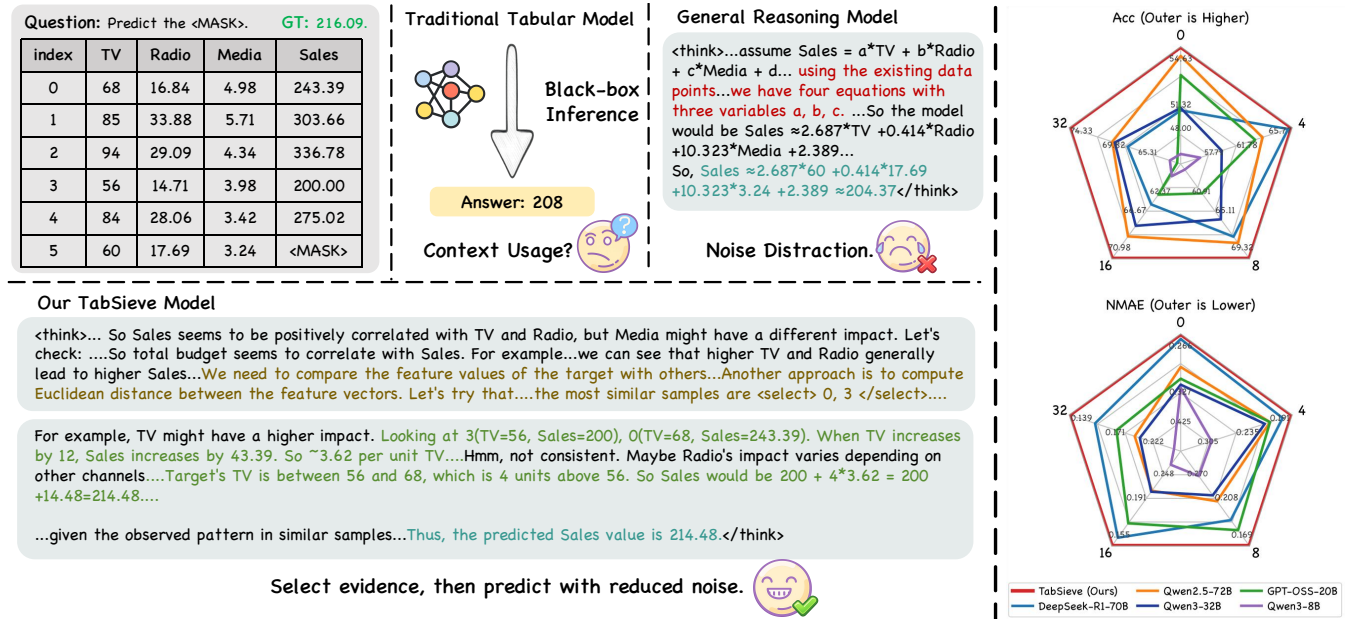


Figure 1: Left: We contrast three prediction paradigms. Traditional models cannot explicitly interpret how context is used. Strong LLMs with in-context prompting can be distracted by **noisy context**. TabSieve first performs **evidence selection** and then conducts **noise-filtered reasoning** to produce the final **prediction**. Right: We compare TabSieve with strong LLM baselines across multiple few-shot settings on both classification and regression tasks.

1 Introduction

Tabular analysis serves as the essential diagnostic foundation for understanding structured data in applications such as climate science, healthcare, finance and energy [1, 4, 10, 26], while tabular

prediction transforms those historical insights into actionable foresight to drive high-stakes decision-making. Unlike isolated instance prediction, real-world tables typically contain other rows that are statistically correlated with the target row. Therefore, in-context learning (ICL) in tabular prediction is vital to achieve robust generalization and stable performance.

*Equal contribution.

However, most existing methods still perform instance-wise inference [2, 17, 23]. This design becomes brittle when transferring across tables whose schemas, column semantics, or data distributions differ. Although recent foundation models incorporate table context, they remain constrained by limited reasoning capabilities for textual metadata and high sensitivity to context composition. Conversely, Large Language Models (LLMs) exhibit strong reasoning and in-context learning capabilities [3, 19] to cast tabular prediction as language modeling by serializing headers and rows into natural language [20, 27, 43]. Naively concatenating a few-shot set into the prompt does not reliably yield controllable gains in practice. Two risks are particularly salient. (i) The model may not reliably condition its predictions on the provided context during inference, particularly for non-reasoning models [8, 37]. (ii) Recent studies suggest that many failures of strong LLMs arise from ignoring contextual details or incorrectly applying the context [12]. In realistic deployments, available demonstrations are often noisy or weakly relevant. The lack of a mechanism to select informative rows can cause the model to rely on unhelpful evidence, resulting in degraded accuracy and robustness [46].

To address these issues, we propose TabSieve, a *select-then-predict* reasoning framework for tabular prediction. As shown in Figure 1, given a table and a query row, TabSieve first analyzes the table structure and column semantics to form an initial hypothesis about the relationship between input features and the target. It then explicitly selects a small set of evidential rows that are most informative for the query and finally predicts the missing value. Compared to passively appending demonstrations, TabSieve turns row selection into a constrained intermediate decision, enabling the model to prioritize high-value evidence under a limited context budget and reducing sensitivity to noisy rows.

To equip the model with these capabilities, we build a rigorous data synthesis pipeline that converts 331 tables from existing collections [43, 44] into a large-scale set of training instances with intermediate reasoning traces. Specifically, we construct a teacher-driven workflow that performs structure understanding and feature analysis, explicitly selects effective reference rows, and then completes the final prediction. By applying strict filtering and rejection sampling to retain only high-quality trajectories, we construct a cold-start supervised dataset TabSieve-SFT-40K that provides direct supervision for both evidence selection and prediction.

Building on this dataset, we further introduce TAB-GRPO for reinforcement learning (RL) by designing separate rewards for evidence selection and prediction to jointly improve selection quality and answer accuracy. In addition, a practical complication in tabular prediction is the coexistence of classification and regression objectives. We observe that in early training, regression tasks often exhibit larger advantage scales, which can dominate the optimization direction and induce early-stage bias. To mitigate this effect, we propose a task-advantage balancing mechanism to adaptively rescale the regression advantages. This rescaling dampens overly strong updates driven by regression at the beginning of training, leading to more stable joint optimization. Our contributions are summarized as follows:

- We propose TabSieve, a reasoning-based tabular predictor that explicitly selects in-table evidence and uses it to support

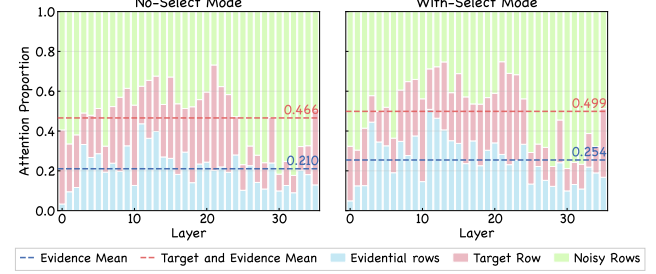


Figure 2: Explicit evidence selection concentrates attention on informative rows.

prediction. We also construct TabSieve-SFT-40K to provide high-quality supervision for evidence selection.

- We introduce TAB-GRPO, a dynamic task-advantage balancing strategy, to mitigate early-stage optimization imbalance between classification and regression.
- We evaluate TabSieve on 75 classification tables and 52 regression tables. TabSieve consistently outperforms baselines, yielding average gains of 2.92% on classification and 4.45% on regression over the second-best method. Further analyses show that context selection increases attention to the selected evidence.

2 Diagnosing the Need to Optimize Tabular In-Context Learning

Previous studies have investigated the role of attention in hallucination and grounding failures, suggesting that insufficient attention allocation to evidential context is a potential factor behind ungrounded outputs [22, 24, 25]. At the same time, several studies indicate that tokens with higher attention weights tend to have a stronger influence on the final decision [11, 14]. Motivated by these observations, in this section, we use attention-based analysis to examine how general LLMs utilize tabular context during prediction. Specifically, we center our study on two research questions:

RQ1: Can introducing an explicit evidence selection declaration in the reasoning trace steer the model’s attention toward evidential rows?

RQ2: If the model is guided to emphasize noisy context, can the context become actively misleading and drive the model to incorrect answers?

2.1 Evidence Focus Improves with an Explicit Selection Trace

We categorize the table rows into target rows, evidential rows, and noisy rows. The target row refers to the query instance. Evidential rows are defined as the rows with high embedding similarity to the target row, while remaining context rows are treated as noise. We then conduct a comparative analysis of the attention allocation of Qwen3-8B [45] to these token groups under two inference modes. In the With-Select mode, before the model produces a prediction, we insert a short evidence-usage declaration into the reasoning trace. This declaration includes a `<select>` block that lists the indices of evidential rows and states that these rows will be used to support the prediction. In the No-Select mode, the model performs standard

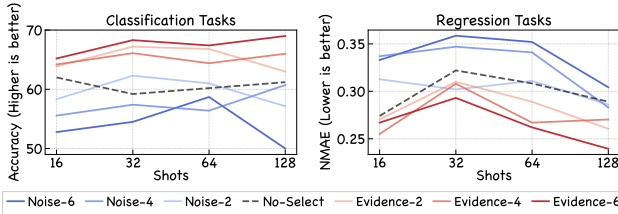


Figure 3: Effect of explicit row selection under evidential or noisy in-table context.

inference and outputs the answer directly, without such an explicit selection trace.

An explicit `<select>` declaration shifts the attention toward evidential rows and away from noisy context. Figure 2 shows the layer-wise attention proportions over table tokens under the two inference modes. Compared with No-Select, attention in With-Select shifts noticeably toward evidential rows. The mean fraction of attention on evidential rows increases from 0.210 to 0.254, and the combined fraction of attention on the target and evidential rows rises from 0.466 to 0.499, accompanied by a corresponding decrease in attention to noisy rows. These results indicate that injecting a lightweight intermediate selection structure encourages the model to concentrate attention on key evidence, mitigating attention dilution from irrelevant context.

2.2 Noisy Context Can Be Actively Misleading Under In-Context Learning

We further evaluate the impact of evidence selection quality on prediction performance. Concretely, we test whether emphasizing irrelevant rows can be actively misleading, rather than simply unhelpful. For shot budgets of 16, 32, 64, and 128, we sample 80 prediction tasks per configuration. Within each task, we label in-context rows as evidence or noise using the same embedding-similarity criterion. We then evaluate three inference settings that differ only in the inserted selection trace: (i) No-Select, which performs standard inference without an explicit selection trace; (ii) Evidence- S , which inserts a `<select>` trace listing S evidential rows and states that they will be used; and (iii) Noise- S , which inserts the same trace and statement but lists S rows sampled from the noisy set.

Selecting noisy rows hurts performance, indicating that irrelevant context can be actively misleading for prediction. As shown in Figure 3, Evidence- S generally improves performance relative to No-Select, whereas Noise- S degrades performance, and the performance gap typically widens as S increases. This suggests that tabular ICL is fragile to noisy context. When the model mistakenly attends to noisy rows, the context can bias the inference and reduce prediction quality. Conversely, concentrating attention on the evidential rows we define leads to higher prediction accuracy. This motivates optimizing tabular ICL so that models can identify valid evidence and concentrate attention on them during prediction.

3 Method

In the above analysis, we observe that tabular ICL exhibits weak evidence focus by default, and inserting an explicit `<select>` trace substantially shifts attention from noisy rows toward evidential rows. We further show that tabular ICL is poorly robust to noisy

context, since treating noise as evidence degrades prediction performance. To address these issues, we propose a two-stage training strategy to train TABSIEVE, as illustrated in Figure 4. We first conduct cold-start initialization on TabSieve-SFT-40K, a synthesized dataset of select-then-predict trajectories. We then perform reinforcement learning with TAB-GRPO to jointly refine evidence selection and improve prediction accuracy. To stabilize early-stage optimization, TAB-GRPO balances task advantages across regression and classification objectives.

3.1 Preliminary

3.1.1 Tabular Prediction Tasks. We consider a labeled tabular dataset $\mathcal{D} = \{(x_i, y_i)\}_{i=1}^N$ with N instances and d feature columns. Each row $x_i = (x_{i1}, \dots, x_{id})$ lies in the instance space $\mathcal{X} = \mathcal{X}_1 \times \dots \times \mathcal{X}_d$ and $y_i \in \mathcal{Y}$ is the target. For C -class classification, $\mathcal{Y} = \{0, 1, \dots, C-1\}$; for regression, $\mathcal{Y} \subseteq \mathbb{R}$. The tabular prediction problem is to learn a predictor $f_\theta : \mathcal{X} \rightarrow \mathcal{Y}$ such that, given a query row $x \in \mathcal{X}$, the model outputs $\hat{y} = f_\theta(x)$.

3.1.2 In-Context Learning for Tabular Data. In the ICL setting, we test on a new tabular task with dataset \mathcal{D}' . Besides a query instance $x^{(q)} \in \mathcal{X}'$, the model is provided with a context set of K labeled examples $C = \{(x^{(k)}, y^{(k)})\}_{k=1}^K \subseteq \mathcal{X}' \times \mathcal{Y}'$, typically drawn from the same table as the query. The model predicts by conditioning on the context $\hat{y}^{(q)} = f_{\theta'}(x^{(q)}, C)$. Equivalently, an ICL predictor implements a mapping $f_{\theta'} : (\mathcal{X}' \times \mathcal{Y}')^K \times \mathcal{X}' \rightarrow \mathcal{Y}'$ with context and adapts to \mathcal{D}' without updating parameters.

3.2 Cold-Start Data Construction

To bootstrap TabSieve with both evidence selection and prediction capability, we construct a cold-start supervised dataset, TabSieve-SFT-40K, which provides explicit signals for the select-then-predict process. Since existing tabular prediction datasets lack chain-of-thought reasoning traces, we build a reasoning corpus from raw tables. Specifically, starting from 331 tables collected by previous methods [43, 44], we first preprocess them into task instances, and then use a teacher-driven workflow to synthesize reasoning trajectories including schema analysis, evidence selection, and prediction.

3.2.1 Data Preprocessing. Before trajectory synthesis, we preprocess raw tables into task instances through target selection, weak correlation feature filtering, and evidence retrieval.

Target Selection. Rather than fixing the target column from the original table, we ask a teacher model to evaluate each column as a candidate prediction target based on its name semantics, data type, and inferability from the remaining columns. To improve reliability, we apply self-consistency with multiple samples and determine the final decision by majority vote. This procedure enables a single table to yield multiple prediction tasks with different targets. It also produces a reverse reasoning trace that reasons from the original target back to its supporting features, strengthening schema understanding beyond surface serialization [6].

Weak Correlation Feature Filtering. To improve training efficiency, we filter weakly related features. Specifically, we first remove the identifier columns, then compute mutual information between each remaining feature and the target. We retain the minimal feature

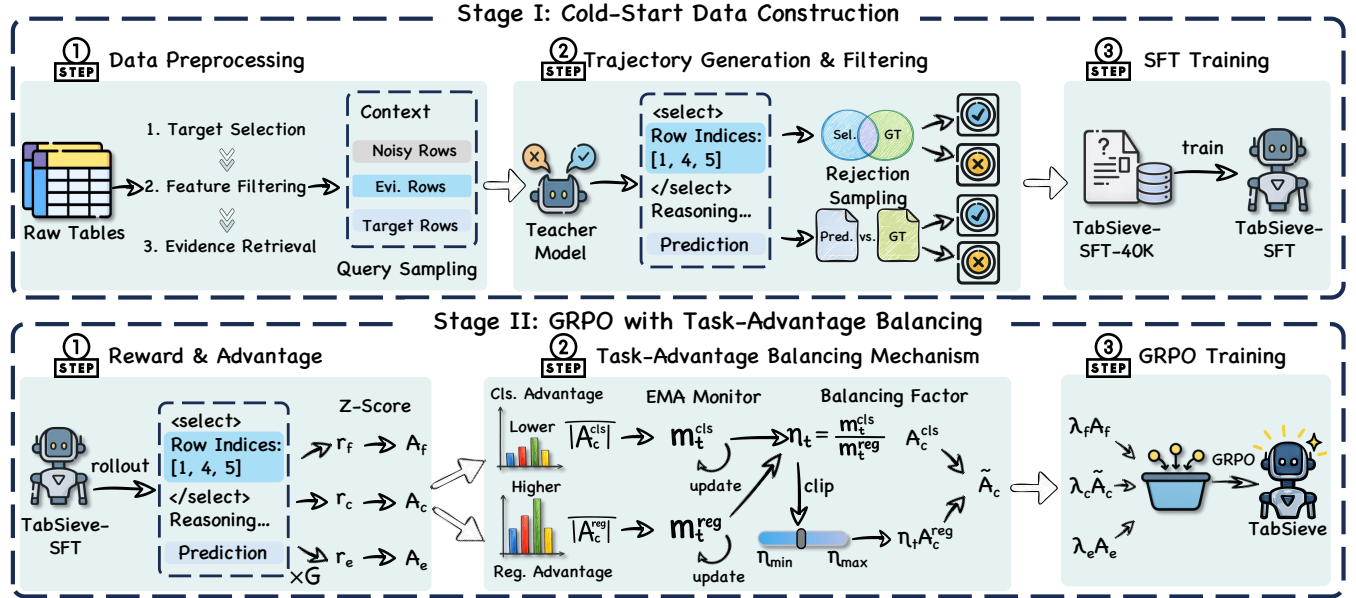


Figure 4: Training pipeline of TabSieve. We construct tabular prediction tasks and synthesize select-then-predict trajectories from a teacher model to build SFT dataset. Starting from the SFT-initialized model, TAB-GRPO extends GRPO with task-advantage balancing to mitigate optimization imbalance and strengthen context selection for robust in-context learning.

subset whose cumulative mutual information exceeds 90%, while enforcing that at least eight feature columns remain. This strategy shortens prompts and improves the signal-to-noise ratio, yet preserves moderate noise so that tasks remain non-trivial and better reflect real-world deployment conditions.

Evidence Retrieval. For each task, we sample a query row and build candidate support sets with size $K \in \{1, 4, 8, 16, 32\}$. To obtain supervised ground truth of the evidence, we compute embeddings for all rows and retrieve the top-32 nearest neighbors of the query row by cosine similarity as an evidence pool. We then populate the K candidates by mixing evidential rows and randomly sampled rows, where the evidence ratio is uniformly sampled from $[0, 0.5]$. The lower bound simulates scenarios where relevant evidence is missing, while the upper bound controls difficulty and prevents overly clean contexts that would make prediction trivially easy.

3.2.2 Trajectory Generation and Filtering. To produce effective supervision signals, we construct a synthesis workflow with a teacher model. The workflow consists of evidential rows selection and target prediction, and both steps are coupled with strict rejection sampling to ensure reliable trajectories.

Evidential Rows Selection. Allowing the teacher to freely choose evidence greatly expands the search space and reduces the success rate. To make the task more tractable, we decompose the procedure into two steps. First, we explicitly inform the teacher that there are exactly E evidential rows among the K candidate context rows, and ask it to interpret the table schema, analyze relationships among features, and select exactly E evidential rows. Second, we prompt the teacher model to rewrite its selection trace, removing any statements that indicate prior knowledge of E , so that the final trajectory does not reveal the number of evidential rows.

Target Prediction. Given an accepted evidence selection trace, the teacher continues to predict the target value. For classification tasks, we keep a sample only if the prediction matches the ground truth exactly. For regression tasks, we first require the prediction to achieve $MAPE < 25\%$. We then prompt the teacher to refine the reasoning so that the final boxed value matches the ground truth exactly. We retry prediction up to five times and discard the instance otherwise. Finally, we remove trajectories with abnormal length and use an LLM-as-judge to filter invalid reasoning traces that exhibit logical leaps or insufficient justification. We use the TabSieve-SFT-40K produced by this pipeline to perform SFT, which provides an effective initialization for subsequent RL training. The distribution of the dataset is provided in Appendix A.2.

3.3 GRPO with Task-Advantage Balancing

We further strengthen TabSieve using reinforcement learning. Our goal is to improve both evidence selection and target prediction under limited and noisy in-table context. We build on Group Relative Policy Optimization (GRPO) [32] and introduce a task-advantage balancing mechanism, which alleviates the early-training imbalance where regression tends to dominate the updates and stabilizes joint learning over classification and regression.

3.3.1 Reward Design and Advantage Computation. For RL training, we construct TabSieve-RL-40K, and the detailed construction procedure is provided in Appendix A.3. Each training instance is a quadruple, denoted by (x, y, E^*, τ) , where x is the input prompt, y is the ground-truth target, E^* is the gold evidence set, and $\tau \in \{\text{cls, reg}\}$ indicates the task type. Given a sampled model output o , we define three reward components:

$$r_f = R_f(x, o), \quad r_e = R_e(x, o, E^*), \quad r_c = R_c(x, o, y, \tau). \quad (1)$$

Format reward. The format reward $R_f(x, o)$ verifies whether o contains a valid evidence-selection block and a boxed answer. Specifically, we parse `<select>...</select>` and `\boxed{·}`. If either parsing step fails, we set $R_f(x, o) = 0$; otherwise $R_f(x, o) = 1$.

Evidence reward. The evidence reward R_e measures the quality of evidence selection. Let $\hat{E}(x, o)$ be the set of selected row indices parsed from `<select>`, and let $E^*(x)$ be the precomputed gold evidence set. We compute precision and recall as:

$$\text{Prec} = \frac{|\hat{E} \cap E^*|}{|\hat{E}| + \varepsilon_F}, \quad \text{Rec} = \frac{|\hat{E} \cap E^*|}{|E^*| + \varepsilon_F}, \quad (2)$$

and define R_e using the F_1 score:

$$R_e(x, o, E^*) = \frac{2 * \text{Prec} * \text{Rec}}{\text{Prec} + \text{Rec} + \varepsilon_F}, \quad (3)$$

where $\varepsilon_F > 0$ is a small constant for numerical stability.

Correctness reward. The correctness reward R_c evaluates quality of the prediction. Let $\hat{y}(x, o)$ be the value parsed from the boxed answer `\boxed{·}`. For classification, we use an exact match:

$$R_c(x, o, y, \text{cls}) = \mathbf{1}[\hat{y}(x, o) = y]. \quad (4)$$

For regression, we apply an exponential shaping based on mean absolute percentage error (MAPE):

$$R_c(x, o, y, \text{reg}) = \exp(-\gamma \cdot \text{MAPE}(\hat{y}(x, o), y)), \quad (5)$$

where $\text{MAPE}(\hat{y}, y) = \frac{|\hat{y} - y|}{|y| + \delta}$ and $\delta > 0$ avoids division by zero.

Advantage Computation. For each prompt x , we sample a group of G candidate outputs $\{o_i\}_{i=1}^G$ from a behavior policy π_{θ^-} . For each reward component $k \in \{f, e, c\}$, we compute a group-relative advantage by whitening rewards within the group:

$$A_i^{(k)} = \frac{r_i^{(k)} - \text{mean}(\{r_1^{(k)}, \dots, r_G^{(k)}\})}{\text{std}(\{r_1^{(k)}, \dots, r_G^{(k)}\}) + \varepsilon_A}, \quad k \in \{f, e, c\}, \quad (6)$$

where $\varepsilon_A > 0$ is a small constant for numerical stability.

3.3.2 Task-Advantage Balancing Mechanism.

Motivation. In mixed-task training, we observe that the *correctness reward* of regression instances increases faster in the early-stage than that of classification instances. We further analyze the *correctness advantages* after the normalization in Eq. (6) and find that regression samples exhibit a larger correctness-advantage magnitude, namely larger $|A^{(c)}|$. In GRPO, policy updates are weighted by advantages, so a larger $|A^{(c)}|$ implies stronger effective optimization strength for the corresponding samples and can make regression dominate the update direction. This imbalance may bias the model toward regression and lead to premature convergence to a regression local optimum before it learns robust behaviors that generalize across both task types.

Balancing factor computation. To mitigate this issue, we estimate the task-wise advantage scale using the mean absolute correctness advantage and construct an adaptive balancing factor. Specifically, we maintain exponential moving averages (EMA) of this quantity for each task type:

$$m_t^u = \beta m_{t-1}^u + (1 - \beta) \mathbb{E}[|A^{(c)}| \mid \tau = u], \quad u \in \{\text{cls, reg}\}, \quad (7)$$

where $\beta \in (0, 1)$ is a decay factor that controls the smoothing of the estimate. Then we compute the balancing factor:

$$\eta(\tau) = \begin{cases} 1, & \tau = \text{cls}, \\ \eta_t, & \tau = \text{reg}, \end{cases} \quad \eta_t = \text{clip}\left(\frac{m_t^{\text{cls}}}{m_t^{\text{reg}} + \varepsilon_B}, \eta_{\min}, \eta_{\max}\right), \quad (8)$$

where $\varepsilon_B > 0$ ensures numerical stability and $0 < \eta_{\min} \leq \eta_{\max} \leq 1$ bounds the scaling. We apply this factor to obtain the balanced correctness advantage:

$$\tilde{A}_i^{(c)} = \eta(\tau) A_i^{(c)}. \quad (9)$$

This factor reduces the optimization gap between classification and regression, enabling stable joint optimization.

GRPO objective. We aggregate the component advantages into a single advantage for optimization:

$$A_i = \lambda_f A_i^{(f)} + \lambda_e A_i^{(e)} + \lambda_c \tilde{A}_i^{(c)}, \quad (10)$$

where $\lambda_f, \lambda_e, \lambda_c$ control the relative importance of each component. Following GRPO, let π_θ be the current policy and define the importance ratio $\rho_i(\theta) = \frac{\pi_\theta(o_i|x)}{\pi_{\theta^-}(o_i|x)}$. The final objective is:

$$\max_{\theta} \mathbb{E} \left[\frac{1}{G} \sum_{i=1}^G \min\left(\rho_i(\theta) A_i, \text{clip}(\rho_i(\theta), 1 - \varepsilon_{\text{low}}, 1 + \varepsilon_{\text{high}}) A_i\right) \right], \quad (11)$$

where ε_{low} and $\varepsilon_{\text{high}}$ are the clipping thresholds.

4 Experiments

4.1 Experimental Setup

4.1.1 Implementation Details. To construct the SFT dataset, we process 331 tables collected from previous works [43, 44]. We use Qwen3-Embedding-8B [47] to encode each table row and Qwen3-Next-80B-Thinking [45] as the teacher model to synthesize trajectories. In the SFT stage, we initialize from Qwen3-8B [45] and fine-tune it with LLaMA-Factory [48]. We use a global batch size of 128, a learning rate of 10^{-4} , and train for 4 epochs. For RL stage, our implementation of TAB-GRPO is based on the VeRL [33] framework¹. We use a batch size of 256 and a learning rate of 10^{-6} , and train for 2 epochs. For each prompt, we sample $G = 8$ rollouts per group. β in EMA is set to 0.99 following the common practice. Additional hyperparameter settings are reported in Appendix A.4.

4.1.2 Evaluation. We evaluate on the benchmark released by GTL and TP-BERTa [43, 44], which contains 75 classification tables and 52 regression tables. To prevent data leakage, we manually filtered out any training tables that also appear in the evaluation benchmark. Following common tabular in-context learning protocols, we report results under multiple shot budgets [5, 20, 27]. For each shot setting, we uniformly sample 5K query rows to form the evaluation set and construct the in-context support set by sampling labeled rows from the same table with three different random seeds. We use accuracy (Acc) for classification and normalized mean absolute error (NMAE) for regression. To reduce evaluation variance in few-shot regression and limit the impact of extreme outliers, we clip the NMAE for each sample at 1.0 before aggregation [43].

¹<https://anonymous.4open.science/r/TabSieve-C634>

Table 1: Classification Results. We report accuracy (\uparrow) averaged over all datasets under zero-shot and few-shot settings. Rank_z denotes the average rank across all datasets in the zero-shot setting, while Rank_i denotes the average rank computed across all datasets and all few-shot settings. Δ denotes the performance gain relative to Qwen3-8B.

Model	size	0	4	8	16	32	Rank_z	Rank_i
Traditional Tabular Models								
LR	–	–	51.39	56.11	61.94	63.38	–	9.28
XGBoost	–	–	49.93	51.79	58.38	62.98	–	10.18
CatBoost	–	–	51.25	56.42	65.88	72.64	–	8.54
STUNT	–	–	47.40	51.44	51.72	53.96	–	12.00
FT-Transformer	–	–	54.31	59.74	68.60	71.45	–	7.92
TabPFN	–	–	52.68	60.70	69.28	73.67	–	7.62
General Large Language Models								
Qwen2.5-72B-Instruct	72B	54.07	63.67	67.95	68.98	70.87	5.29	5.91
DeepSeek-R1-Distill-Llama-70B	70B	51.04	65.52	67.39	66.06	69.62	5.67	6.64
QwQ-32B	32B	52.07	64.11	62.46	65.62	67.07	5.84	8.10
Qwen3-32B	32B	51.18	60.74	65.84	68.01	70.67	5.61	6.19
GLM-4-32B-0414	32B	54.06	63.73	66.45	68.21	68.99	5.52	6.78
GPT-OSS-20B	20B	53.05	63.14	63.53	65.17	65.59	5.73	8.08
Qwen3-8B	8B	48.18	58.77	60.91	63.01	65.67	7.19	9.10
Llama-3.1-8B-Instruct	8B	38.32	46.77	48.88	48.02	47.50	8.65	13.09
Mistral-7B-Instruct-v0.3	7B	45.94	57.18	55.78	54.37	53.82	6.39	10.23
Tabular Large Language Models								
TableLLM-13B	13B	30.09	40.20	41.60	39.74	33.31	9.03	12.80
Tabula-8B	8B	39.92	41.77	41.62	44.13	42.70	8.48	14.10
TableGP2-7B	7B	36.29	41.84	43.62	45.99	47.93	9.24	13.71
TabSieve (Ours)	8B	54.63	65.77	69.32	70.98	74.33	5.25	5.31
Δ over base model		+6.45	+7.00	+8.42	+7.97	+8.65	-1.93	-3.79

Table 2: Regression Results. We report normalized mean absolute error (NMAE \downarrow) averaged over all datasets under zero-shot and few-shot settings. Rankings are computed per dataset and then averaged across datasets.

Model	size	0	4	8	16	32	Rank_z	Rank_i
Traditional Tabular Models								
LR	–	–	0.348	0.348	0.342	0.339	–	10.05
XGBoost	–	–	0.237	0.200	0.184	0.160	–	7.89
CatBoost	–	–	0.235	0.192	0.179	0.158	–	7.23
FT-Transformer	–	–	0.363	0.363	0.357	0.354	–	11.21
TabPFN	–	–	0.228	0.186	0.165	0.144	–	6.32
General Large Language Models								
Qwen2.5-72B-Instruct	72B	0.297	0.206	0.205	0.198	0.178	4.57	6.93
DeepSeek-R1-Distill-Llama-70B	70B	0.270	0.197	0.188	0.160	0.152	4.33	6.24
QwQ-32B	32B	0.293	0.220	0.196	0.164	0.158	4.36	6.49
Qwen3-32B	32B	0.317	0.210	0.211	0.197	0.182	5.71	7.96
GLM-4-32B-0414	32B	0.303	0.214	0.191	0.188	0.182	5.81	7.38
GPT-OSS-20B	20B	0.310	0.206	0.180	0.170	0.165	4.71	6.93
Qwen3-8B	8B	0.325	0.268	0.239	0.235	0.222	5.76	8.65
Llama-3.1-8B-Instruct	8B	0.567	0.351	0.338	0.331	0.319	10.19	12.96
Mistral-7B-Instruct-v0.3	7B	0.668	0.416	0.405	0.370	0.364	10.86	13.44
Tabular Large Language Models								
TableLLM-13B	13B	0.709	0.476	0.581	0.571	0.541	10.52	15.07
Tabula-8B	8B	0.648	0.420	0.395	0.382	0.445	11.05	14.52
TableGP2-7B	7B	0.511	0.504	0.473	0.477	0.508	9.14	15.64
TabSieve (Ours)	8B	0.266	0.192	0.169	0.158	0.139	3.86	5.85
Δ over base model		-0.059	-0.076	-0.071	-0.078	-0.082	-1.90	-2.81

Baselines. Our baselines fall into three categories: *Traditional Tabular Models*, *General Large Language Models*, and *Tabular Large Language Models*. For traditional tabular learning, we include logistic regression, XGBoost [7] and CatBoost [30], and stronger neural tabular approaches including STUNT [28], FT-Transformer [17], and TabPFN [21]. Except for TabPFN, all other tabular predictors are fine-tuned on the labeled data for each dataset. We report their performance starting from the few-shot regime rather than the zero-shot setting. For general LLMs, we evaluate a diverse set of models spanning different scales, covering DeepSeek-R1-Distill-Llama-70B [19], Qwen2.5-72B-Instruct [38], QwQ-32B [39], Qwen3-32B [45], GPT-OSS-20B [29], GLM-4-32B-0414 [16], Qwen3-8B [45], Llama-3.1-8B-Instruct [13], and Mistral-7B-Instruct-v0.3 [9].

These models are tested under a unified prompting protocol across $K \in \{0, 4, 8, 16, 32\}$. For tabular-specialized LLMs, we consider Tabula [15], TableLLM [20], and TableGPT2 [36], which are trained or adapted explicitly for table understanding or tabular prediction. For these tabular LLMs, we follow the prompting templates and input formatting used in the official implementations.

4.2 Main Results

Tables 1 and 2 report the performance of all methods on classification and regression tasks, respectively. Overall, TabSieve achieves the best overall performance on both task types and consistently improves as the shot budget increases. On classification, TabSieve

attains 54.63% accuracy in the zero-shot setting and increases to 74.33% at 32-shot, achieving the best average rank in both the zero-shot and few-shot regimes. On regression, TabSieve reduces NMAE from 0.266 to 0.139 and again ranks first overall. Averaged over all shot budgets, TabSieve improves performance over the second-best baseline by 2.92% on classification and 4.45% on regression, which highlights the improved in-context learning capability of TabSieve.

Comparison to traditional tabular models. Traditional tabular predictors rely on task-specific fitting on labeled data and are therefore not applicable in the zero-shot setting. In contrast, TabSieve relies on table schema semantics and the general knowledge encoded in the language model, allowing it to generalize well across tables without task-specific training. As the shot budget grows, tabular predictors can fit within-table patterns from sufficient labeled rows and improve performance. In particular, TabPFN reaches performance comparable to TabSieve at 32-shot. However, TabSieve still substantially outperforms traditional tabular models in terms of the average rank over few-shot settings, indicating that its gains are not confined to a single high-shot point but persist across different shot budgets. Overall, TabSieve shows stronger generalization and robustness in few-shot settings, while matching the best conventional baselines when sufficient labeled context is provided.

Comparison to general LLMs. TabSieve consistently outperforms all evaluated general LLMs, even those with up to 70B parameters. At 32-shot, TabSieve reaches 74.33% accuracy on classification and 0.139 NMAE on regression, exceeding the strongest general LLMs by clear margins. Compared with the base Qwen3-8B, TabSieve delivers substantial gains on both tasks, and these improvements typically become more pronounced as the shot budget increases. This pattern indicates that TabSieve can exploit context more effectively. Its select-then-predict procedure prioritizes evidential rows and suppresses noisy context, resulting in stable and favorable scaling as more shots are provided. In contrast, several LLMs exhibit non-monotonic performance as K grows, suggesting a higher sensitivity to noisy context.

Comparison to tabular LLMs. TabSieve substantially outperforms prior tabular LLMs by large margins. We attribute this improvement to the fact that TabSieve is explicitly trained for tabular reasoning, which enhances its ability to reason over in-table evidence and translate that reasoning into more accurate predictions. In contrast, existing tabular LLMs typically lack strong reasoning capability and do not provide an explicit chain-of-thought, which makes them generalize less reliably under heterogeneous schemas and task distributions. Moreover, TabSieve learns to filter contextual rows through the selection step, which makes it particularly effective in in-context learning settings where demonstrations can be noisy.

4.3 Ablation Study

In this section, we conduct ablations on the training stages, key RL components, and the evidence selection. We report the mean results averaged over zero-shot and all few-shot configurations.

Training stages. Figure 5 summarizes the incremental gains from SFT and RL stage. Starting from the backbone QWEN3-8B, SFT on TabSieve-SFT-40K (+SFT) yields a clear improvement, showing

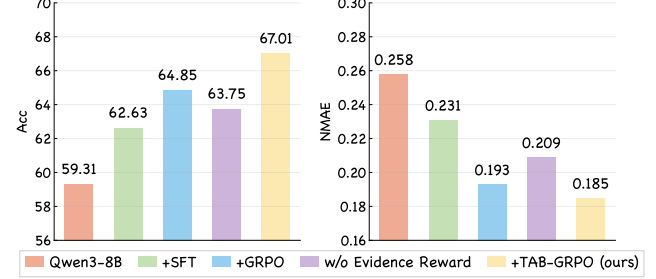


Figure 5: Ablation on training stages and RL components.

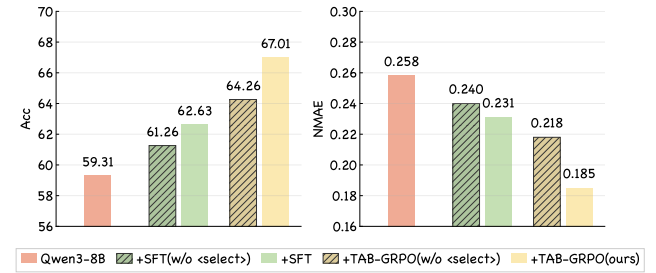


Figure 6: Ablation on evidence selection.

that the synthesized reasoning trajectories provide an effective initialization. Standard GRPO (+GRPO) further improves both tasks, indicating that our reward design provides a reliable optimization signal that effectively refines the selection policy and reinforces prediction quality beyond pure imitation.

RL components. Figure 5 also reports an ablation over key RL components. Removing the evidence reward (w/o Evidence Reward) leads to a clear degradation. This result further indicates that explicitly optimizing evidence selection strengthens the model’s context-filtering capability, which is essential for improving in-context learning performance beyond answer-level optimization. In addition, replacing vanilla GRPO with our TAB-GRPO yields a large improvement in classification. This gain supports our task-advantage balancing design, which effectively alleviates the optimization imbalance in the early-stage training and leads to a more stable joint optimization over classification and regression tasks.

Evidence selection. Figure 6 quantifies the contribution of explicit evidence selection by removing the selection process from the SFT dataset. Specifically, we construct SFT(w/o <select>) by deleting the <select> step in the synthesized trajectories and fine-tuning the backbone on this modified dataset. The resulting model performs worse than the full SFT model, indicating that the gain is not solely due to supervising the prediction procedure, but also comes from evidence selection. This further highlights the importance of evidence selection for in-context learning. We then continue RL training on top of SFT(w/o <select>) while disabling the evidence reward, yielding TAB-GRPO(w/o <select>). Although RL still improves the model over its SFT initialization, this variant remains consistently weaker than TabSieve. These results suggest that explicit evidence selection is a key capability to unlock the full benefits of the select-then-predict framework.

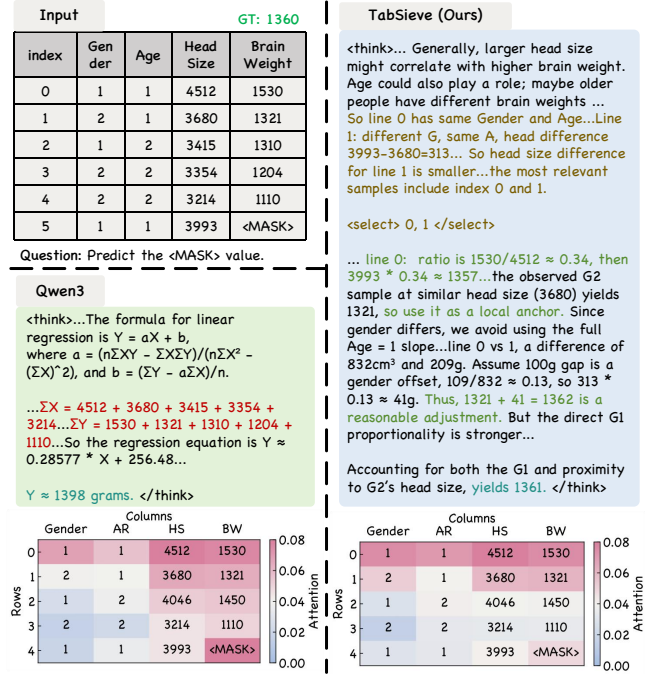


Figure 7: Case Study of Evidence Selection and Attention.

4.4 Benefits of Evidence Selection Analysis

We provide a case study to highlight how evidence selection improves robustness to noisy in-table context, as shown in Figure 7. Without evidence selection, Qwen3-8B fits a linear model over all of the contextual rows. In the few-shot regime with sparse context, such global fitting is highly susceptible to noisy or weakly relevant rows, which can lead to large prediction errors. In contrast, TabSieve follows a select-then-predict procedure that first identifies a small subset of informative rows and predicts conditioned on the selected evidence. By filtering out less relevant rows, TabSieve reduces the influence of noise and encourages evidence-grounded reasoning, resulting in a better prediction.

We further visualize the attention distribution over table tokens following prior work [40]. Concretely, we extract attention weights from the final 12 transformer layers during inference and aggregate them to obtain a cell-level heatmap over the table. As illustrated at the bottom of Figure 7, Qwen3-8B allocates broadly distributed attention across the context, assigning high attention to the HS and BW fields in every contextual row, which increases the chance of being influenced by irrelevant or noisy rows. Moreover, it assigns substantial attention to the masked target value, even though this entry contains no information. In contrast, TabSieve shows a markedly more concentrated attention pattern, allocating much larger attention mass to the selected rows. This alignment between the explicit selection trace and the attention distribution suggests that evidence selection not only improves accuracy, but also makes context usage more interpretable and auditable. Additional case studies are provided in Appendix B.

5 Related Works

Deep Learning Models for Tabular Data. Tabular prediction has long been a central problem in machine learning. Gradient-boosted decision trees have historically been strong performers, and prior studies show that tree ensembles often remain highly competitive and outperform many deep models [18, 34]. To narrow this gap, researchers have proposed attention-based neural architectures to better capture feature interactions in tabular data, including TabNet [2], FT-Transformer [17], and SAINT [35]. Beyond single table learning, cross-table generalization methods address schema heterogeneity and knowledge transfer. TransTab leverages column metadata alongside cell values to improve table understanding [42], while XTab and TP-BERTa explore shared modeling components and value tokenization schemes to strengthen transfer across diverse schemas [44, 49]. Despite these advances, most deep tabular models follow an instance-wise inference paradigm and do not exploit within-table evidence during inference. In-context learning models further highlight the potential of context-aware inference, where predictions are produced by conditioning on a set of labeled rows within the table at test time [21, 31].

Large Language Models for Tabular Prediction. Large language models have recently gained traction for tabular prediction due to their in-context learning and reasoning abilities. Early works serialize tables into text and rely on prompting to elicit predictions [20, 27]. Later studies emphasize improving data quality and training signals to better adapt LLMs to heterogeneous tables. MediTab rewrites structured clinical records into natural language descriptions through a dedicated data engine and uses the resulting data to train the model [41]. GTL converts large-scale tabular corpora into instruction style templates and performs continued pre-training to enhance generalization [43]. Tabula builds large transfer data and fine-tunes open-source LLMs with table-aware attention, improving both zero-shot and few-shot performance [15]. TabR1 further explores optimization beyond supervised learning by introducing reinforcement learning [5]. Despite these developments, context usage in most existing LLM-based approaches is still largely implicit and heavily dependent on prompt designs, which can be brittle when the context budget is limited and demonstrations are noisy. In contrast, TabSieve makes evidence selection an explicit intermediate action and jointly optimizes it with prediction, enabling more reliable suppression of noisy contextual rows and more consistent use of few-shot evidence in in-context learning.

6 Conclusion

In this paper, we propose TabSieve, a *select-then-predict* framework for tabular prediction that makes in-table evidence usage explicit. Instead of passively concatenating demonstrations, TabSieve selects a small set of informative rows as evidence and then performs prediction conditioned on the selected rows, which focuses the context budget on salient evidence and reduces sensitivity to noisy rows. To train this behavior, we construct TabSieve-SFT-40K through synthesis and strict filtering, and propose TAB-GRPO to stabilize training on mixed regression and classification tasks. Extensive experiments across diverse tabular prediction settings show that TabSieve focuses on salient in-table evidence and achieves competitive performance against strong general and tabular baselines across

different shot budgets. Despite these gains, there remain several directions to improve. First, due to computational constraints, we only explored TabSieve at the 8B scale. Scaling to larger backbones and broader training budgets is an important next step. Second, future work can strengthen TabSieve by collecting more tables from diverse sources and converting them into larger training corpora, which may improve generalization to heterogeneous schemas.

Acknowledgments

To Robert, for the bagels and explaining CMYK and color spaces.

References

- [1] Peter Martinec Addo, Dominique Guegan, and Bertrand Hassani. 2018. Credit risk analysis using machine and deep learning models. *Risks* 6, 2 (2018), 38.
- [2] Sercan Ö Arik and Tomas Pfister. 2021. Tabnet: Attentive interpretable tabular learning. In *Proceedings of the AAAI conference on artificial intelligence*, Vol. 35. 6679–6687.
- [3] Tom Brown, Benjamin Mann, Nick Ryder, Melanie Subbiah, Jared D Kaplan, Prafulla Dhariwal, Arvind Neelakantan, Pranav Shyam, Girish Sastry, Amanda Askell, et al. 2020. Language models are few-shot learners. *Advances in neural information processing systems* 33 (2020), 1877–1901.
- [4] Salva Röhling Cachay, Venkatesh Ramesh, Jason NS Cole, Howard Barker, and David Rolnick. 2021. ClimART: A benchmark dataset for emulating atmospheric radiative transfer in weather and climate models. *arXiv preprint arXiv:2111.14671* (2021).
- [5] Pengxiang Cai, Zihao Gao, and Jintai Chen. 2025. TabR1: Taming GRPO for tabular reasoning LLMs. *arXiv preprint arXiv:2510.17385* (2025).
- [6] Justin Chen, Zifeng Wang, Hamid Palangi, Rujun Han, Sayna Ebrahimi, Long Le, Vincent Perot, Swaroop Mishra, Mohit Bansal, Chen-Yu Lee, et al. 2025. Reverse thinking makes llms stronger reasoners. In *Proceedings of the 2025 Conference of the Nations of the Americas Chapter of the Association for Computational Linguistics: Human Language Technologies (Volume 1: Long Papers)*. 8611–8630.
- [7] Tiangi Chen. 2016. XGBoost: A Scalable Tree Boosting System. *Cornell University* (2016).
- [8] Xiang Cheng, Chengyan Pan, Minjun Zhao, Deyang Li, Fangchao Liu, Xinyu Zhang, Xiao Zhang, and Yong Liu. 2025. Revisiting Chain-of-Thought Prompting: Zero-shot Can Be Stronger than Few-shot. *arXiv preprint arXiv:2506.14641* (2025).
- [9] Chanyeol Choi, Junseong Kim, Seolhwa Lee, Jihoon Kwon, Sangmo Gu, Yejin Kim, Minkyung Cho, and Jy-yong Sohn. 2024. Linq-embed-mistral technical report. *arXiv preprint arXiv:2412.03223* (2024).
- [10] Grace Colverd, Ronita Bardhan, and Jonathan Cullen. 2025. Machine learning methods for domestic energy prediction and retrofit potential for small-neighbourhoods at national scales in England and Wales. *Energy and Buildings* (2025), 116388.
- [11] Jay DeYoung, Sarthak Jain, Nazneen Fatema Rajani, Eric Lehman, Caiming Xiong, Richard Socher, and Byron C Wallace. 2020. ERASER: A benchmark to evaluate rationalized NLP models. In *Proceedings of the 58th annual meeting of the association for computational linguistics*. 4443–4458.
- [12] Shihao Dou, Ming Zhang, Zhangyue Yin, Chenhao Huang, Yujiong Shen, Junzhe Wang, Jiayi Chen, Yuchen Ni, et al. 2026. CL-bench: A Benchmark for Context Learning. *arXiv:2602.03587 [cs.CL]* <https://arxiv.org/abs/2602.03587>
- [13] Abhimanyu Dubey, Abhinav Jauhri, Abhinav Pandey, Abhishek Kadian, Ahmad Al-Dahle, Aiesha Letman, Akhil Mathur, Alan Schelten, Amy Yang, Angela Fan, et al. 2024. The llama 3 herd of models. *arXiv e-prints* (2024), arXiv-2407.
- [14] Brage Eilertsen, Røksva Bjørgfinsdóttir, Francinelle Vargas, and Ali Ramezani-Kebrya. 2025. Aligning Attention with Human Rationales for Self-Explaining Hate Speech Detection. *arXiv preprint arXiv:2511.07065* (2025).
- [15] Josh Gardner, Juan C Perdomo, and Ludwig Schmidt. 2024. Large scale transfer learning for tabular data via language modeling. *Advances in Neural Information Processing Systems* 37 (2024), 45155–45205.
- [16] Team GLM, Aohan Zeng, Bin Xu, Bowen Wang, Chenhui Zhang, Da Yin, Dan Zhang, Diego Rojas, Guanyu Feng, Hanlin Zhao, et al. 2024. Chatglm: A family of large language models from glm-130b to glm-4 all tools. *arXiv preprint arXiv:2406.12793* (2024).
- [17] Yury Gorishniy, Ivan Rubachev, Valentin Khrulkov, and Artem Babenko. 2021. Revisiting deep learning models for tabular data. *Advances in neural information processing systems* 34 (2021), 18932–18943.
- [18] Léo Grinsztajn, Edouard Oyallon, and Gaël Varoquaux. 2022. Why do tree-based models still outperform deep learning on typical tabular data? *Advances in neural information processing systems* 35 (2022), 507–520.
- [19] Daya Guo, Dejian Yang, Haowei Zhang, Junxiao Song, Ruoyu Zhang, Runxin Xu, Qihao Zhu, Shirong Ma, Peiyi Wang, Xiao Bi, et al. 2025. Deepseek-r1: Incentivizing reasoning capability in llms via reinforcement learning. *arXiv preprint arXiv:2501.12948* (2025).
- [20] Stefan Heggelmann, Alejandra Buendia, Hunter Lang, Monica Agrawal, Xiaoyi Jiang, and David Sontag. 2023. Tabllm: Few-shot classification of tabular data with large language models. In *International conference on artificial intelligence and statistics*. PMLR, 5549–5581.
- [21] Noah Hollmann, Samuel Müller, Katharina Eggensperger, and Frank Hutter. 2022. Tabpfn: A transformer that solves small tabular classification problems in a second. *arXiv preprint arXiv:2207.01848* (2022).
- [22] Qidong Huang, Xiaoyi Dong, Pan Zhang, Bin Wang, Conghui He, et al. 2024. Opera: Alleviating hallucination in multi-modal large language models via over-trust penalty and retrospection-allocation. In *Proceedings of the IEEE/CVF Conference on CVPR*. 13418–13427.
- [23] Xin Huang, Ashish Khetan, Milan Cvitkovic, and Zohar Karnin. 2020. Tabtransformer: Tabular data modeling using contextual embeddings. *arXiv preprint arXiv:2012.06678* (2020).
- [24] Fushuo Huo, Wenchao Xu, Zhong Zhang, Haozhao Wang, Zhicheng Chen, and Peilin Zhao. 2024. Self-introspective decoding: Alleviating hallucinations for large vision-language models. *arXiv preprint arXiv:2408.02032* (2024).
- [25] Chengzhi Liu, Zhongxing Xu, Qingyue Wei, Juncheng Wu, James Zou, et al. 2025. More Thinking, Less Seeing? Assessing Amplified Hallucination in Multimodal Reasoning Models. *arXiv preprint arXiv:2505.21523* (2025).
- [26] Zheng Liu, Wenqi Shu, Teng Li, Xuan Zhang, and Wei Chong. 2025. Interpretable machine learning for predicting sepsis risk in emergency triage patients. *Scientific Reports* 15, 1 (2025), 887.
- [27] Jaehyun Nam, Woomin Song, Seong Hyeon Park, Jihoon Tack, Sukmin Yun, Jaehyung Kim, Kyn Hwan Oh, and Jinwoo Shin. 2024. Tabular transfer learning via prompting llms. *arXiv preprint arXiv:2408.11063* (2024).
- [28] Jaehyun Nam, Jihoon Tack, Kyungmin Lee, Hankook Lee, and Jinwoo Shin. 2023. Stunt: Few-shot tabular learning with self-generated tasks from unlabeled tables. *arXiv preprint arXiv:2303.00918* (2023).
- [29] OpenAI. 2025. gpt-oss-120b & gpt-oss-20b Model Card. *arXiv:2508.10925 [cs.CL]* <https://arxiv.org/abs/2508.10925>
- [30] Liudmila Prokhorenkova, Gleb Gusev, Aleksandr Vorobev, Anna Veronika Dorgush, and Andrey Gulin. 2018. CatBoost: unbiased boosting with categorical features. *Advances in neural information processing systems* 31 (2018).
- [31] Jingang Qu, David Holzmaßer, GaÄTl Varoquaux, and Marine Le Morvan. 2025. Tabicl: A tabular foundation model for in-context learning on large data. *arXiv preprint arXiv:2502.05564* (2025).
- [32] Zhihong Shao, Peiyi Wang, Qihao Zhu, Runxin Xu, Junxiao Song, Xiao Bi, et al. 2024. Deepseekmath: Pushing the limits of mathematical reasoning in open language models. *arXiv preprint arXiv:2402.03300* (2024).
- [33] Guangming Sheng, Chi Zhang, Zilingfeng Ye, Xibin Wu, Wang Zhang, et al. 2024. HybridFlow: A Flexible and Efficient RLHF Framework. *arXiv preprint arXiv:2409.19256* (2024).
- [34] Ravid Shwartz-Ziv and Amitai Armon. 2022. Tabular data: Deep learning is not all you need. *Information Fusion* 81 (2022), 84–90.
- [35] Gowthami Somepalli, Micah Goldblum, Avi Schwarzschild, C Bayan Bruss, and Tom Goldstein. 2021. Saint: Improved neural networks for tabular data via row attention and contrastive pre-training. *arXiv preprint arXiv:2106.01342* (2021).
- [36] Aofeng Su, Aowen Wang, Chao Ye, Chen Zhou, Ga Zhang, Guangcheng Zhu, Haobo Wang, Haokai Xu, Hao Chen, Haoze Li, Haoxuan Lan, Jiaming Tian, et al. 2024. TableGPT2: A Large Multimodal Model with Tabular Data Integration. *arXiv:2411.02059 [cs.LG]* <https://arxiv.org/abs/2411.02059>
- [37] Hao Sun, Chenming Tang, Gengyang Li, and Yunfang Wu. 2025. Lost in the Passage: Passage-level In-context Learning Does Not Necessarily Need a "Passage". *arXiv preprint arXiv:2502.10634* (2025).
- [38] Qwen Team. 2024. Qwen2.5: A Party of Foundation Models. <https://qwenlm.github.io/blog/qwen2.5/>
- [39] Qwen Team. 2025. QwQ-32B: Embracing the Power of Reinforcement Learning. <https://qwenlm.github.io/blog/qwq-32b/>
- [40] Songjiao Tu, Qichao Zhang, Jingbo Sun, Yuqian Fu, Linjing Li, Xiangyuan Lan, Dongmei Jiang, Yaowei Wang, and Dongbin Zhao. 2025. Perception-Consistency Multimodal Large Language Models Reasoning via Caption-Regularized Policy Optimization. *arXiv preprint arXiv:2509.21854* (2025).
- [41] Zifeng Wang, Chufan Gao, Cao Xiao, and Jimeng Sun. 2023. Meditab: Scaling medical tabular data predictors via data consolidation, enrichment, and refinement. *arXiv preprint arXiv:2305.12081* (2023).
- [42] Zifeng Wang and Jimeng Sun. 2022. Transtab: Learning transferable tabular transformers across tables. *Advances in Neural Information Processing Systems* 35 (2022), 2902–2915.
- [43] Xumeng Wen, Han Zhang, Shun Zheng, Wei Xu, and Jiang Bian. 2024. From supervised to generative: A novel paradigm for tabular deep learning with large language models. In *Proceedings of the 30th ACM SIGKDD Conference on Knowledge Discovery and Data Mining*. 3323–3333.
- [44] Jiahuan Yan, Bo Zheng, Hongxia Xu, Yiheng Zhu, Danny Z Chen, Jimeng Sun, Jian Wu, and Jintai Chen. 2024. Making pre-trained language models great on

tabular prediction. *arXiv preprint arXiv:2403.01841* (2024).

- [45] An Yang, Anfeng Li, Baosong Yang, Beichen Zhang, Binyuan Hui, Bo Zheng, Bowen Yu, Chang Gao, Chengan Huang, Chenxu Lv, et al. 2025. Qwen3 technical report. *arXiv preprint arXiv:2505.09388* (2025).
- [46] Feipeng Zhang, Wenyu Jiang, Jun Shu, Feng Zheng, Hongxin Wei, et al. 2024. On the noise robustness of in-context learning for text generation. *Advances in Neural Information Processing Systems* 37 (2024), 16569–16600.
- [47] Yanzhao Zhang, Mingxin Li, Dingkun Long, Xin Zhang, Huan Lin, Baosong Yang, et al. 2025. Qwen3 Embedding: Advancing Text Embedding and Reranking Through Foundation Models. *arXiv preprint arXiv:2506.05176* (2025).
- [48] Yaowei Zheng, Richong Zhang, Junhao Zhang, Yanhan Ye, Zheyuan Luo, Zhangchi Feng, and Yongqiang Ma. 2024. Llamafactory: Unified efficient fine-tuning of 100+ language models. *arXiv preprint arXiv:2403.13372* (2024).
- [49] Bingzhao Zhu, Xingjian Shi, Nick Erickson, Mu Li, George Karypis, and Mahsa Shoaran. 2023. Xtab: Cross-table pretraining for tabular transformers. *arXiv preprint arXiv:2305.06090* (2023).

A Implementation Details.

A.1 Details of Feature Filtering

We consider a labeled tabular dataset $\mathcal{D} = \{(x_i, y_i)\}_{i=1}^N$ with N instances and d feature columns. We first discard identifier-like columns, such as user IDs or email addresses, since their near-unique values can spuriously yield high mutual information with the target and dominate MI-based ranking, despite being uninformative for prediction. After this removal, we retain d' candidate feature columns. We denote the j -th remaining feature column as a random variable X_j and the target column as Y . For each candidate feature X_j , we compute its MI score with the target as:

$$s_j = I(X_j; Y) = \sum_u \sum_v p(u, v) \log \frac{p(u, v)}{p(u)p(v)}, \quad (12)$$

where u and v enumerate possible values of X_j and Y , respectively.

We then rank features by MI scores in descending order, obtaining $s_{(1)} \geq \dots \geq s_{(d')}$. We select the smallest prefix whose cumulative MI reaches a fixed fraction ρ of the total MI mass:

$$m^* = \min \left\{ m \left| \sum_{t=1}^m s_{(t)} \geq \rho \sum_{t=1}^{d'} s_{(t)} \right. \right\}, \quad \rho = 0.9. \quad (13)$$

To avoid over-pruning, we enforce a minimum retained feature budget:

$$m^* \leftarrow \max(m^*, m_{\min}), \quad m_{\min} = 8. \quad (14)$$

Finally, we keep the top- m^* features together with the target column to form the filtered table. This procedure removes weakly related fields and improves the signal-to-noise ratio, while maintaining diverse dependency patterns and moderate residual noise that better reflects real-world tabular prediction scenarios.

A.2 Distribution of TabSieve-SFT-40K

We summarize the data distribution of our SFT dataset in Figure 8. After strict trajectory filtering, TabSieve-SFT-40K contains 41,083 select-then-predict trajectories. As shown in the left panel, each instance is constructed under a shot budget $K \in \{0, 4, 8, 16, 32\}$ and belongs to either a classification or a regression task. Across the five shot budgets, the dataset contains 9,610, 10,228, 9,064, 8,365, and 3,816 instances, corresponding to 23.4%, 24.9%, 22.1%, 20.4%, and 9.3%. The task types are approximately balanced overall, and both types are present under every shot budget. For $K > 0$, we further report the evidence ratio r , defined as the fraction of evidential rows among the sampled in-context candidates. As shown in the right panel of Figure 8, r ranges from 0 to 0.5 with an average value of $\bar{r} = 0.261$. The histogram exhibits a broad coverage of evidence densities, including both sparse-evidence cases and relatively dense-evidence cases, which improves distributional diversity and better reflects realistic tabular prediction scenarios where useful context can be sparse and unevenly distributed.

A.3 Reinforcement Learning Dataset Construction

We build the reinforcement learning training set TabSieve-RL-40K by filtering instances that can destabilize optimization or provide limited learning signal. We first discard examples for which the teacher model fails to produce an acceptable prediction within five

Table 3: Core SFT hyperparameters for cold-start.

Hyperparameters	Value
Epochs	4.0
Micro batch size	4
Gradient accumulation	4
Learning rate	1×10^{-4}
Warmup ratio	0.1
Learning rate scheduler	Cosine
GPUs	$8 \times \text{H200}$
Training time (h)	14.11

Table 4: Core RL hyperparameters for TAB-GRPO.

Hyper-parameters	Value
Epochs	2.0
Train batch size	256
Rollout Sampling Num	8
Rollout temperature	1.0
KL coefficient	0.001
Learning rate	1×10^{-6}
Max prompt length	4096
Max response length	5120
Clip ratio (low) ϵ_{low}	0.2
Clip ratio (high) ϵ_{high}	0.28
λ_f	0.1
λ_e	0.2
λ_c	0.7
γ	1.0
β	0.99
η_{\min}	0.8
η_{\max}	1.0
GPUs	$8 \times \text{H200}$
Training time (h)	25.08

attempts during SFT trajectory synthesis, as these cases often indicate insufficient supporting evidence, excessive difficulty, or an ill-posed target. We further remove examples that Qwen3-8B [45] solves correctly with a single forward evaluation. Since Qwen3-8B shares the same pretraining knowledge as our backbone, such instances are typically near-trivial and yield limited benefit from reinforcement learning. After filtering, TabSieve-RL-40K concentrates on medium difficulty instances, which improves training stability and makes the learning signal more informative.

A.4 Parameters Setup

We report the key hyperparameters used in our two-stage training pipeline, and present the essential settings for SFT and RL training with TAB-GRPO in Table 3 and Table 4, respectively. Omitted options follow the default values of the training framework.

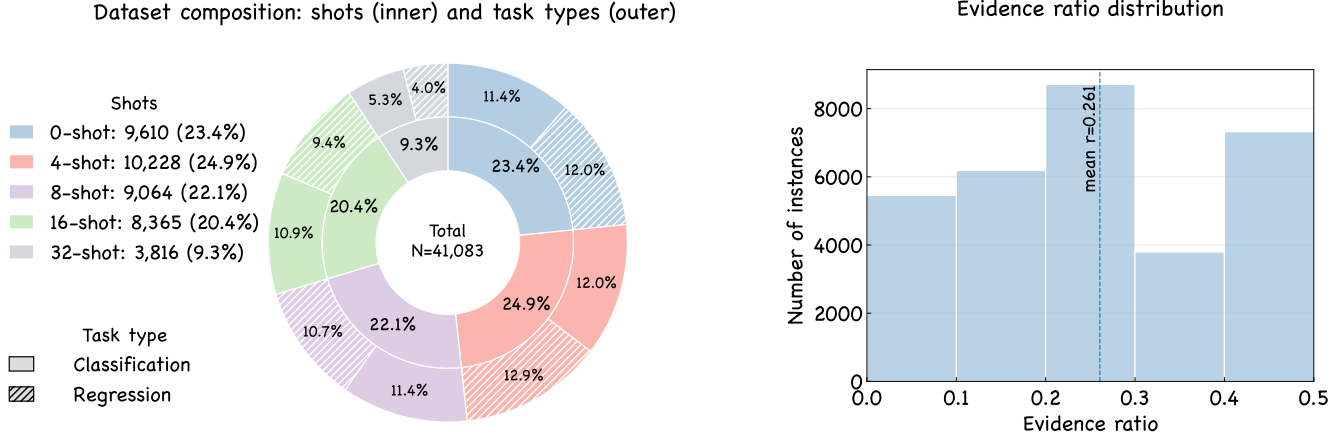


Figure 8: Data distribution of the SFT dataset. Left: dataset composition across the five shot budgets, with each slice further decomposed into classification and regression trajectories. Right: distribution of the evidence ratio for $K > 0$.

A.5 Prompt Template

Prompt Template	
System:	
# Role	You are an expert in Data Mining and Logical Reasoning. Your core expertise lies in deeply comprehending the intrinsic logic of tabular data, analyzing the structural and feature-target dependencies, identifying samples similar to the target, and utilizing these insights to predict the '[MISSING]' value.
# Task Description	
Given a sampled sub-table and its metadata:	<ul style="list-style-type: none"> The last cell of the final row is marked as '[MISSING]', serving as the prediction target. You must conduct a step-by-step analysis within '<think>' tags, adhering to the 'Reasoning Requirements', to derive a specific predicted value.
# Reasoning Requirements	<ul style="list-style-type: none"> Comprehend the table structure and the semantics of feature columns. Analyze potential relationships between features and the target (e.g., strong correlations, causality). Identify samples similar to the target. During the reasoning process, enclose the indices of these selected samples within '<select>' tags (e.g., '<select> 2, 4, 7 </select>'). Synthesize the analysis to model the logic connecting features to the target and predict the '[MISSING]' value. Construct a complex and comprehensive logical derivation from features to the target, simulating a predictive model. Reject lazy reasoning: Deriving the result solely by calculating the mean, median, or mode of similar samples is strictly prohibited.
# Output Format	

Output ONLY the final answer, excluding any additional text, and put your final answer within '`\boxed{}`'.

User:

```
## Metadata of the table named <name of the table>
<metadata of the table>
## Sampled Sub-table
<sub-table>
## Candidate Values
<range of the target value>
Please reason step by step, output ONLY the final answer, put your final answer within \boxed{}.
```

Case Study (Zero-Shot in Classification Tasks)	
Question	index 215
## Metadata of the table named stroke-prediction-dataset.	gender Female
The column 'age' represents 'Age of the individual in years' and is a 'numerical' variable.	age 79.0
...	hypertension 0
## Sampled Sub-table	heart_disease 1
...	ever_married No
## Candidate Values	work_type Private
The possible values are: '1', '0'.	Residence_type Urban
Please reason step by step, output	avg_glucose_level 205.33
ONLY the final answer, put your final answer within <code>\boxed{}</code> .	bmi 31.0
Ground Truth: 1	smoking_status smokes
	stroke [MISSING]
<think> Okay, let's tackle this problem step by step...Now, considering the relationships between features and the target. Based on general knowledge, stroke risk factors typically include hypertension (high blood pressure), heart disease, smoking... For example, hypertension is a major risk factor for stroke. Similarly, having a heart disease could increase the risk...</think>	
Stroke risk factors include age (older age increases risk), heart disease (yes), smoking, high glucose (diabetes), BMI (obesity), etc...However, heart disease is present. Also, smoking is a risk factor. High glucose could indicate diabetes, which is a risk factor. Age 79 is very high risk...	
Given that heart disease is a strong predictor of stroke, and she has it, and she smokes, the risk is elevated. High glucose further increases this risk. Therefore, despite no hypertension, the overall risk is high, and the most probable outcome is stroke=1. </think>	

Figure 9: Zero-shot case in classification tasks.

Case Study (Zero-Shot in Regression Tasks)			
Question			
<pre>## Metadata of the table named cern-electron-collision-data. The column 'E1' represents 'Energy of electron 1' and is a 'numerical' variable. The column 'px1' represents 'Momentum of electron 1 in the x direction'... ## Sampled Sub-table ... ## Candidate Values The value of M ranges from 2.00008 to 109.999 (inclusive). Please reason step by step, output **ONLY** the final answer, put your final answer within \boxed{.}.</pre>			
Ground Truth: 34.4543			
<pre><think> Okay, let's tackle this problem step by step. First, let's look at the metadata... In physics, the invariant mass of a system is calculated from the total energy and momentum. For two particles, the formula is $M = \sqrt{(E1 + E2)^2 - (p_{x1} + p_{x2})^2 - (p_{y1} + p_{y2})^2 - (p_{z1} + p_{z2})^2}$...</pre>			
<pre>Since there are no other samples available for comparison, no samples can be selected. <select></select></pre>			
<pre>...So the answer should be the computed value of M using the formula. Let's compute it for the given row... First, sum of energies: $E1 + E2 = 86.0024 + 3.70897 = 89.71137...$ Now, compute the sum of squared momenta: $(p_{x1} + p_{x2})^2 = (-1.3353026)^2 \approx 1.7830...$ Total sum of squared momenta: $1.7830 + 206.72 + 6652.54 \approx 6861.043...$ Then $M^2 = 8048.140 - 6861.046 = 1187.097$ $M = \sqrt{1187.097} \approx 34.454$</pre>			
<pre>This value falls within the expected range of 2.00008 to 109.999, confirming the calculation is consistent. Therefore, the missing value is approximately 34.454. </think></pre>			

Figure 10: Zero-shot case in regression tasks.

Case Study (Few-Shot)																																																														
Question																																																														
<pre>## Metadata of the table named go-to-college-dataset. The column 'type_school' represents 'The type of school the student attends, either Academic or Vocational' and is a 'categorical' variable...</pre>																																																														
## Sampled Sub-table																																																														
<table border="1"> <thead> <tr> <th>index</th><th>type_school</th><th>accreditation</th><th>gender</th><th>interest</th><th>reside_nce</th><th>parent_salary</th><th>parent_was_in_college</th><th>will_go_to_college</th></tr> </thead> <tbody> <tr> <td>779</td><td>Vocational</td><td>B</td><td>Male</td><td>Less Interested</td><td>Rural</td><td>6710000</td><td>True</td><td>True</td></tr> <tr> <td>771</td><td>Vocational</td><td>B</td><td>Female</td><td>Interested</td><td>Urban</td><td>3580000</td><td>False</td><td>False</td></tr> <tr> <td>438</td><td>Academic</td><td>A</td><td>Male</td><td>Less Interested</td><td>Urban</td><td>4180000</td><td>False</td><td>False</td></tr> <tr> <td>569</td><td>Academic</td><td>B</td><td>Male</td><td>Very Interested</td><td>Urban</td><td>6640000</td><td>False</td><td>True</td></tr> <tr> <td>91</td><td>Vocational</td><td>B</td><td>Male</td><td>Interested</td><td>Urban</td><td>3240000</td><td>False</td><td>[MISSING]</td></tr> </tbody> </table>									index	type_school	accreditation	gender	interest	reside_nce	parent_salary	parent_was_in_college	will_go_to_college	779	Vocational	B	Male	Less Interested	Rural	6710000	True	True	771	Vocational	B	Female	Interested	Urban	3580000	False	False	438	Academic	A	Male	Less Interested	Urban	4180000	False	False	569	Academic	B	Male	Very Interested	Urban	6640000	False	True	91	Vocational	B	Male	Interested	Urban	3240000	False	[MISSING]
index	type_school	accreditation	gender	interest	reside_nce	parent_salary	parent_was_in_college	will_go_to_college																																																						
779	Vocational	B	Male	Less Interested	Rural	6710000	True	True																																																						
771	Vocational	B	Female	Interested	Urban	3580000	False	False																																																						
438	Academic	A	Male	Less Interested	Urban	4180000	False	False																																																						
569	Academic	B	Male	Very Interested	Urban	6640000	False	True																																																						
91	Vocational	B	Male	Interested	Urban	3240000	False	[MISSING]																																																						
<pre>## Candidate Values The possible values are: 'True', 'False'.</pre>																																																														
<pre>Please reason step by step, output ONLY the final answer, put your final answer within \boxed{.}.</pre>																																																														
Ground Truth: False																																																														
<pre><think> Okay, let's tackle this problem step by step. The task is to predict the missing information in the 'will_go_to_college' column for the target sample... Let's think about general knowledge first. Typically, the type of school... urban vs rural could have different access to college resources. Parent's salary might indicate financial ability to afford college. If the parent was in college, maybe that's a positive indicator for the student to go too... </pre>																																																														
<pre>Line 771: Vocational, B... So same school type (Vocational), same school accreditation (B)... But maybe gender isn't a strong factor here. So line 771 is very similar... Line 569: Academic, B... So same gender (Male), same school accreditation (B), similar interest (Very Interested vs Interested), same residence (Urban), parent not in college. Parent salary higher. So maybe this is the second similar... <select> 771, 569 </select></pre>																																																														
<pre>Line 771 has the same school type... The only difference is gender, but gender might not be a strong predictor. For example, line 438 is male... So gender might not be a major factor here... So maybe for Vocational, if parent not in college, they don't go to college. So target would be False. But line 569 is Academic, B... but went True... So school type and salary matter.</pre>																																																														
<pre>So for the target, which is Vocational, B, parent not in college. So maybe target is False. </think></pre>																																																														

Figure 11: Few-shot case in classification tasks.

B More Case Studies

In this section, we present additional examples to illustrate the reasoning patterns of TabSieve under different inference settings.

Figure 9 and Figure 10 show TabSieve in the zero-shot regime. Since no examples are available for in-context learning, the model relies entirely on general knowledge to model relationships among the features and predicts the missing value based on the inferred mapping. Figure 11 presents a few-shot example, where the model first infers and constructs feature relations from the context, then selects a small set of evidential rows, and finally uses the selected evidence to produce the final prediction.